Hum Genet (2014) 133:1419–1429
DOI 10.1007/s00439-014-1475-8

ORIGINAL INVESTIGATION

Identification of a homozygous splice site mutation in the dynein axonemal light chain 4 gene on 22q13.1 in a large consanguineous family from Pakistan with congenital mirror movement disorder

Iltaf Ahmed · Kirti Mittal · Taimoor I. Sheikh · Nasim Vasli · Muhammad Arshad Rafiq · Anna Mikhailov · Mehrnaz Ohadi · Huda Mahmood · Guy A. Rouleau · Attya Bhatti · Muhammad Ayub · Myriam Srour · Peter John · John B. Vincent

Received: 4 April 2014 / Accepted: 23 July 2014 / Published online: 7 August 2014

Abstract Mirror movements (MRMV) are involuntary movements on one side of the body that mirror voluntary movements on the opposite side. Congenital mirror movement disorder is a rare, typically autosomal-dominant disorder, although it has been suspected that some sporadic cases may be due to recessive inheritance. Using a linkage analysis and a candidate gene approach, two genes have been implicated in congenital MRMV disorder to date: *DCC* on 18q21.2 (MRMV1), which encodes a netrin receptor, and *RAD51* on 15q15.1 (MRMV2), which is involved in the maintenance of genomic integrity. Here, we describe a large consanguineous Pakistani family with 11 cases of congenital MRMV disorder reported across five generations, with autosomal recessive inheritance likely. Sanger sequencing of *DCC* and *RAD51* did not identify a mutation. We then employed microarray genotyping and autozygosity mapping to identify a shared region of homozygosity-by-descent among the affected individuals. We identified a large autozygous region of ~3.3 Mb on chromosome 22q13.1 (Chr22:36605976−39904648). We used Sanger sequencing to exclude several candidate genes within this region, including *DMC1* and *NPTXR*. Whole exome sequencing was employed, and identified a splice site mutation in the dynein axonemal light chain 4 gene, *DNAL4*. This splice site change leads to skipping of exon 3, and omission of 28 amino acids from DNAL4 protein. Linkage analysis using Simwalk2 gives a maximum Lod score of 6.197 at this locus. Whether or how DNAL4 function may relate to the function of DCC or RAD51 is not known. Also, there is no suggestion of primary ciliary dyskinesis, *situs inversus*, or defective sperm in affected family

Electronic supplementary material The online version of this article (doi:10.1007/s00439-014-1475-8) contains supplementary material, which is available to authorized users.

I. Ahmed · K. Mittal · T. I. Sheikh · N. Vasli · M. A. Rafiq · A. Mikhailov · M. Ohadi · H. Mahmood · J. B. Vincent (✉)
Molecular Neuropsychiatry and Development (MiND) Lab, Centre For Addiction and Mental Health, Campbell Family Mental Health Research Institute, R32, 250 College Street, Toronto, ON M5T 1R8, Canada
e-mail: john_vincent@camh.net; john.vincent@camh.ca

I. Ahmed · A. Bhatti · P. John
Atta-ur-Rehman School of Applied Biosciences (ASAB), National University of Sciences and Technology (NUST), Islamabad, Pakistan

T. I. Sheikh · J. B. Vincent
Institute of Medical Science, University of Toronto, Toronto, ON, Canada

G. A. Rouleau
Montreal Neurological Institute and Hospital, McGill University, Montreal, QC, Canada

M. Ayub
Division of Developmental Disabilities, Department of Psychiatry, Queen's University, Kingston, ON, Canada

M. Srour
Division of Pediatric Neurology, Departments of Neurology/Neurosurgery, Montreal Children's Hospital-McGill University Health Centre, Montreal, QC, Canada

M. Srour
Division of Pediatric Neurology, Department of Pediatrics, Montreal Children's Hospital-McGill University Health Centre, Montreal, QC, Canada

J. B. Vincent
Department of Psychiatry, University of Toronto, Toronto, ON, Canada

members, which might be anticipated given a putative role for DNAL4 in axonemal-based dynein complexes. We suggest that DNAL4 plays a role in the cytoplasmic dynein complex for netrin-1-directed retrograde transport, and in commissural neurons of the corpus callosum in particular. This, in turn, could lead to faulty cross-brain wiring, resulting in MRMV.

Introduction

Mirror movements (MRMV) were first recorded by Erlenmeyer in 1879, but coined by Cohen et al. (1991), and refer to involuntary contralateral movements mirroring the intended limb movement. MRMV can be found in young children and gradually disappears, typically within the first decade of life; it is presumed that MRMV is a necessary developmental stage in the maturating motor network (Bonnet et al. 2010). If mirror movement persists after the first decade of life with no additional clinical features it is referred to as congenital MRMV. Congenital MRMV is a rare disorder that is mainly inherited in an autosomal-dominant fashion although it has been suggested that some sporadic cases may be caused by recessive forms (Rasmussen 1993).

MRMV may be present in all limbs but it is predominantly found in forelimbs, in muscles controlling the fingers and hands, and their intensity increases with the complexity of the voluntary movement. Consequently, MRMV impairs the ability of an affected individual to perform tasks requiring skilled bimanual coordination such as tying shoelaces, cutting vegetables, or buttoning shirts, etc., which more often than not, is associated with pain in the upper limbs during sustained manual activities. A severe form of congenital MRMV affecting both hands and forearms, was reported in a 15-year-old girl which was caused by multiple and structural abnormalities of the motor network and altered decussation of the corticospinal tract (Regli et al. 1967; Cincotta et al. 2003; Galléa et al. 2011).

MRMV is genetically heterogeneous in nature; heterozygous mutations in *DCC* (deleted in colorectal carcinoma [MIM 120470]), have been reported in families with autosomal-dominant congenital MRMV (MRMV1 [MIM 157600]). The *DCC* gene encodes for a receptor for netrin 1 (NTN1 [MIM 601614]). Impairment of DCC/netrin 1 signaling, which promotes attraction and guidance of developing axons toward the midline, results in alterations of axonal fiber crossing and abnormal ipsilateral connections (Srour et al. 2010; Depienne et al. 2011). DCC has also been shown to co-localize with and form complexes with translation machinery components in neuronal axons and dendrites, and a mechanism is suggested for translational regulation with the spatial precision necessary for axon guidance (Tcherkezian et al. 2010).

Depienne et al. (2012) reported a heterozygous truncating mutation in the *RAD51* gene [MIM 179617] in a large French family with congenital MRMV with incomplete penetrance (MRMV2 [MIM614508]). A second truncating mutation in the *RAD51* gene was identified in a German family with MRMV2. The authors concluded that haploinsufficiency was the pathogenic mechanism, yet the mechanism linking *RAD51* deficiency to the disorder remains unclear. It has been suggested that insufficient RAD51-related DNA repairs during early corticogenesis may lead to excessive apoptosis and altered CNS development (Depienne et al. 2012). A role for RAD51 in axonal guidance is currently not known, although a recent study showed that MRMV patients with *RAD51* mutations have abnormal decussation of the corticospinal tract, abnormal interhemispheric inhibition and bilateral activation of primary motor areas during intended unimanual movements, and abnormal involvement of the supplementary motor area while performing unimanual or bimanual movements (Gallea et al. 2013). Here, we present the genetic analysis of a large consanguineous family from Sindh province in Pakistan with an apparently recessive form of congenital MRMV.

Materials and methods

Patients

The approval for the study was obtained from Institute Review Board and Ethical Committee of Centre for Addiction and Mental Health in Toronto, Canada and the National University of Science and Technology, Islamabad, Pakistan. Families were visited at their homes and were informed about the study. Written informed consent was obtained from participants, or their parents, if under 16 years, for their participation in this study and for photography/videography. The diagnosis of congenital MRMV was carried out according to the guidelines provided by Erlenmeyer (Cohen et al. 1991). The age of patients ranged from 4 to 39 years. The differences in MRMV were also examined with distal extremity movement (first dorsal interossei and flexor digitorum communis) and proximal extremity as well as right and left side. The amplitude of mirroring was also taken in account. Position of major organs in the abdomen and thorax was evaluated by ultrasound for individuals VI:2, VI:8 and VI:15 at a commercial diagnostic ultrasound facility in Sukkur, Sindh Province. 5 ml of blood was drawn for genetic studies in EDTA tubes for DNA extraction, 5 ml using acid-citrate dextrose (ACD) tubes for Epstein-Barr virus transformation to generate lymphoblastoid cell lines, and 3 ml of blood was collected

in Tempus™ Blood RNA Tube (Life Technologies, Carlsbad, CA) for RNA and expression studies.

Whole genome homozygosity-by-descent mapping

DNA was isolated from the blood samples of affected and unaffected individuals by method described previously by Lahiri et al. (1992) with minor modification. PCR amplification of *DCC* and *RAD51* exons was performed (primer sequences indicated in Supplementary Materials), followed by Sanger sequencing through The Centre for Applied Genomics (TCAG, Toronto, Ontario) for affected individuals, but did not reveal any mutations. Genome-wide homozygosity mapping of five affected individuals (V:15, VI:2, V:9, IV:7 and IV:8) and one unaffected family member (V:14) was performed with Gene chip Mapping CytoScan HD array (Affymetrix, CA) at the TCAG facility. Genotypes were analyzed for homozygosity-by-descent (HBD) or autozygous regions using Chromosome Analysis Suite (ChAS; Affymetrix) and HomozygosityMapper (http://www.homozygositymapper.org; Seelow et al. 2009; see Fig. 1).

Copy number variation analysis

In order to ensure that heterozygous copy number mutation of *DCC* or *RAD51* (which may have been missed by Sanger or whole exome methods) was not contributing to the phenotype under a dominant model with incomplete penetrance, we analyzed the CytoScan HD array (Affymetrix, CA) using Chromosome Analysis Suite (ChAS; Affymetrix). We also used this approach to check for any other CNVs present in the affected but not in the unaffected individuals, either heterozygous for dominant or homozygous for recessive. Validation of calls of interest was performed by quantitative real-time PCR, using SYBR® Green based real-time quantitative PCR (qPCR) and a minimum of two independent primer pairs (See Supplementary Table 1). Real-time PCR was run using the ViiA™7 (Life Technologies). All reactions were run in triplicate. The relative standard curve method was used to analyze the CNVs in affected individuals and unaffected relatives using a panel of DNAs from a series of healthy adult comparison individuals (screened for absence of psychiatric illness) as controls. The experimental data were analyzed with ViiA™7 Software v1.1.

Linkage analysis

Microsatellite markers were used to corroborate autozygosity, and the markers D22S280, D22S283, D22S423 and D22S274 were genotyped for DNAs from all available family members. Genotyping was performed at TCAG. Linkage analysis was performed using SimWalk2 (version 2.91) (Sobel and Lange 1996; Sobel et al. 2001, 2002).

Whole exome sequencing

Whole exome sequencing of one affected individual (VI:2) was carried out with the SOLiD 5500 (Life Technologies) platform and TargetSeq exome (Life Technologies) capture array, according to the manufacturers' recommended protocols. The raw reads were aligned using SHRiMP2 (David et al. 2011). Duplicated reads were removed with the MarkDuplicate subroutine of PICARD (http://picard.sourceforge.net). To improve the consensus base resolution, a re-alignment was performed using the SRMA program (Homer and Nelson 2010). Genome Analysis Tool Kit package (GATK; McKenna et al. 2010) was used for Q score recalibration. The resulting BAM files were then annotated using both softwares, DNASTAR (Seqman NGen ver 3.0.4) and ANNOVAR (http://www.openbioinformatics.org/annovar/; Wang et al. 2010) against the human reference genome, build hg19. The detailed reports were exported for further analyses, and filtering for homozygous coding or splice variants that are not known SNPs (dbSNP131) or common alleles reported in 1000 Genomes (http://browser.1000genomes.org/index.html) or in the NHLBI Exome Variant Server (http://evs.gs.washington.edu/EVS/), and the HBD regions were checked for adequate coverage of exons. In addition, WES reads for all genes within HBD regions were checked using the Integrated Genomics Viewer (IGV; www.broadinstitute.org/). For all exons within the HBD regions for which coverage was insufficient (<8×), primers were designed and PCR followed by Sanger sequencing was used in order to exclude these exons. Sanger sequencing was used to confirm a homozygous variant in intron 3 of the gene *DNAL4* within the splice donor canonical consensus "GT" sequence using primers spanning exon 3 [forward: 5′ GGA ACA GGG GCC ACT TTA TT; reverse: 5′ TTA CCC CTG CCC TGT CTC TA; chr22:39176858−39177035 (hg19)]. A cohort of 13 unrelated individuals from Canada with congenital MRMV were screened for mutations in *DNAL4* by PCR followed by Sanger sequencing of the three coding exons (see Supplementary Material for PCR primers). Of the 13 individuals, 2 had familial, autosomal-dominant congenital MRMV disorder and 11 were simplex cases. Sanger sequencing of *DCC* and *RAD51* in all 13 cases did not identify any rare variants. DNAs from 250 Pakistani control individuals was screened for presence of the *DNAL4* variant by PCR (see Supplementary Materials for primers) followed by restriction digestion with the enzyme BsrDI (New England Biolabs, Ipswich, MA). BsrDI is predicted to cut at the site generated by the variant allele.

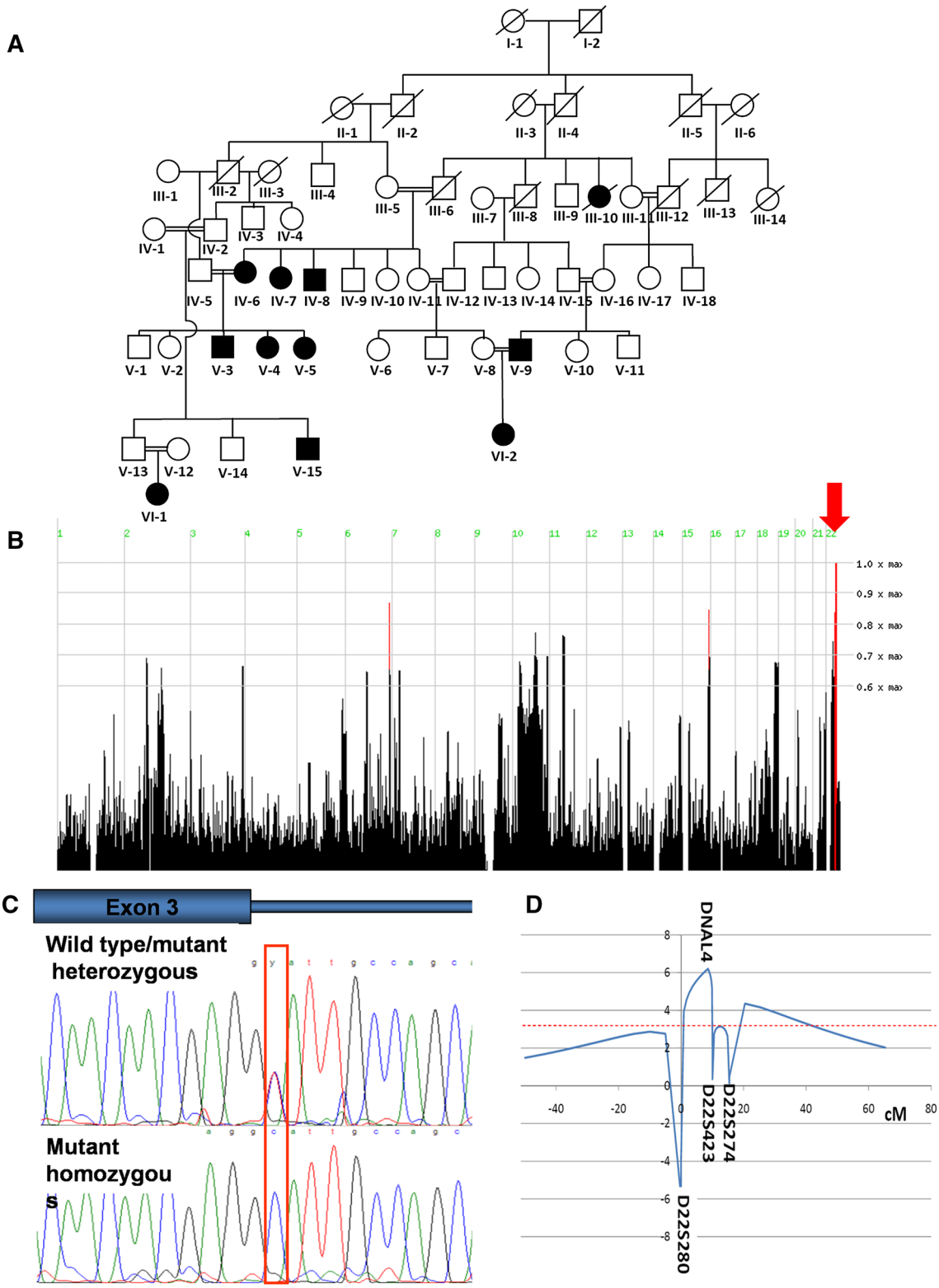

RNA extraction, cDNA synthesis, reverse transcription (RT)-PCR and sequencing

RT-PCR of whole blood or lymphoblast mRNA, followed by Sanger sequencing was used to examine the effects of the *DNAL4* variant on mRNA splicing. Whole blood mRNA from affected MRMV family members V:15 and IV:7 and unaffected individual III:5, was extracted from blood collected in Tempus™ RNA tubes (Life Technologies, Carlsbad, CA) using Trizol. In addition, blood

◀ **Fig. 1** **a** Pedigree of Pakistani MRMV family. Affected individuals are indicated by *dark-shaded symbols*. Affected individuals IV:7, IV:8, V:3, V:15, and VI:2, and unaffected individual V:14 were included in the microarray analysis. **b** Homozygosity Mapper output, showing maximum HBD (across all affected, but not the unaffected individual) only on chromosome 22 (indicated by *red arrow*). The *y* axis indicates the fraction of the maximum homozygosity score (1.0). **c** Ideogram indicating location of the NM_005740.2 c.153+2T>C variant at the intron 3 donor splice site, and electropherograms showing the forward strand heterozygous wild type/mutant sequence and the homozygous mutant (c.153+2T>C) sequence. **d** Linkage analysis using SIMWALK2. Position in Haldane cM is plotted on the *x* axis, and location score (assuming no heterogeneity; $\alpha = 1.0$) on the *y* axis. The significance threshold for linkage of 3.0 is indicated by the *red dashed line*. Maximum location score of 6.197 was achieved for the *DNAL4* c.153+2T>C variant and microsatellite marker D22S423

samples from affected family members V:15, IV:7 and unaffected family member V:11 were collected in acid-citrate-dextrose (ACD) BD Vacutainer® blood tubes (Becton, Dickinson and Company) were diluted (1:1) with Roswell Park Memorial Institute (RPMI) medium, and white blood cells separated using ACCUSPIN tubes (Sigma), and transformed with Epstein-Barr Virus. mRNA was extracted from lymphoblast cells using the TRIzol method. cDNA was synthesized through reverse transcription of 1 µg of RNA using Superscript III™ Reverse Transcriptase (Invitrogen, Carlsbad, CA) and random hexamers according to manufacturer's guidelines. Splicing of *DNAL4* mRNA from the affected and unaffected family members and an unrelated unaffected control was checked by RT-PCR followed by Sanger sequencing using the primers 5′-CCTGAATCTCC TGGGTGTGT and 5′-GAAAAACCAGGACCTGCCTA (from exons 1 and 4 respectively).

Results

A large Pakistani family segregating congenital MRMV disorder was identified and ascertained for genetic studies. The pedigree is complex; however, it would appear that autosomal recessive inheritance is the most likely model of transmission (Fig. 1a). Mirror movements were exclusively and predominantly observed in fingers and hands. Proximal upper limbs were unaffected. The amplitude of movement for the mirroring was generally less compared with the voluntary activity. Furthermore, amplitude of mirroring was noticed equally in the fingers of the right and left hands. Affected individuals could partially suppress these movements. MRMV was absent in the lower limbs. No other neurological or behavioral abnormality was noticed in the affected individuals. Pain and/or cramping during sustained manual activity was not reported by affected individuals. Anosmia and hypogonadism (reported in Kallman syndrome; MIM 308700) were not present in the family members, and reproduction is not affected (see pedigree in Fig. 1a). *Situs inversus* was not present in tested affected family members VI:2, IV:8 and V:15. Also, there was no history of chronic sinusitis, bronchitis, frequent pneumonias, colds, ear infections, or decreased or absent pulmonary mucociliary clearance in any of the affected family members. Typically, onset of symptoms was noted at around 2–3 years of age; however, in some cases, symptoms were reported (anecdotally) to be present much earlier, from 2 to 3 months (e.g. in the offspring of individuals IV:5 and IV:6). Sanger sequencing of known dominant genes for MM (*RAD51* and *DCC*) did not identify a mutation. Microarray analysis for CNVs (see Supplementary Table 2) using ChAS identified a putative deletion of *DCC* exon 22 in just individual IV:7 (affected), but not in any other genotyped affecteds. Quantitative real-time PCR did not validate this loss CNV in IV:7 or in any family members.

Analysis of microarray genotype data indicated a ~3.3 Mb HBD region on chromosome 22q13.1 (Chr22:36605976−39904648; hg19; Fig. 1b). Several smaller HBD regions were also identified (Table 1). NGen (DNASTAR) and ANNOVAR analysis of aligned WES reads identified very few homozygous coding variants not present in dbSNP build 131 (excluding synonymous amino acid substitutions). WES statistics are given in Table 2. More than 98 % of exons within the HBD regions (Table 1) were adequately covered by WES, and the remaining exons were Sanger sequenced in order to completely exclude their involvement. We also confirmed that WES homozygous synonymous changes within the HBD regions are not predicted to result in a cryptic splice event using the splice site prediction algorithm http://www.fruitfly.org/seq_tools/splice.html. WES identified a potential donor splice site mutation two nucleotides within intron 3 of the dynein axonemal light chain 4 gene, *DNAL4*: chr22:39176929A>G; NM_005740.2 (DNAL4_vNM_005740): c.153+2T>C. This substitution destroys the canonical "GT" splice donor site (Figs. 1c, 2a), and the aforementioned splice site prediction algorithm indicates a shift in score from 0.78 (out of 1) for the wild-type mRNA to <0.01 for the mutant. RT-PCR and sequencing of mRNA from lymphocytes and lymphoblasts showed that the result of this splice mutation is skipping of exon 3 (Fig. 2b, c). Exon 2 splices directly to exon 4, maintaining the same reading frame. This alternative splicing was observed only for family members with the c.153+2T>C variant, and was not seen in controls. The removal of exon 3 results in an open reading frame of just 77 amino acid residues (a predicted size of 8.75 kDa) instead of 105 amino acids (12 kDa), effectively a deletion of 28 amino acids (residues 24–51 inclusive). See Fig. 2d and e for protein 3D structure predictions for wild-type and mutant DNAL4, respectively.

Table 1 All HBD regions (hg19) determined by ChAS analysis for affected MRMV family members IV:7, IV: 8, V:9, V:15, and VI:2, in comparison to unaffected individual V:14 (See Fig. 1a), using filter cut-off of ≥100 markers and ≥1 Mb

HBD regions: genomic coordinates (hg19)	Size (Kb)	No. of variants	Mean × coverage	Ref position	Gene	DNASTAR/NGen: base change/amino acid change	ANNOVAR: base change/amino acid change	IGV? (No. of reads)	ConDel
Chr5:45356105−46383335	1,027	0	NA			None	None		
Chr7:62461703−63633799	1,172	19	14			None	None		
Chr8:99806627−101011774	1,205	4	17			None	None		
Chr9:112861714−114922067	2,060	57	16	113169968	SVEP1	c.7912C>T; p. D2638 N	c.7912C>T; p. D2638 N	Y (42)	Neutral
Chr10:21762499−22912743	1,150	7	17	None					
Chr10:81172703−82301802	1,129	62	22	81928835	ANXA11	c.451T>C; p. T151A	c.451T>C; p. T151A	Y (51)	Neutral
Chr16:33591003−34796531	1,206	51	30	None					
Chr22:36605976−39904648	3,299	195	15	38483174	BAIAP2L2	c.1216A>T; p.S406T	c.T1216A:p.S406T	Y (82)	Neutral
				39176929	**DNAL4**		**exon4:c.153+2T>C**	**Y (31)**	
				39418880	APOBEC3D	c.71A>G; p. E24G	c. .71A>G; p. E24G	Y (112)	Neutral

The DNAL4 mutation is indicated in bold

Number of variants per HBD region and mean fold (×) coverage are listed. Homozygous coding variants from DNASTAR NGen analysis and ANNOVAR analysis of WES data for VI:2 are shown, excluding synonymous and SNPs with variant frequency >0.05 (hg1000). Integrated genome viewer (IGV) was used to confirm the variant. For amino acid substitutions, we used Condel—an integrated analysis that uses prediction from five different algorithms, including PolyPhen2, SIFT, and Mutation Assessor (González-Pérez and López-Bigas 2011)

NA not available

This variant was not in any SNP databases, including dbSNP build 138, nor present in 1000 Genomes (http://browser.1000genomes.org/index.html; accessed Jan 2014) or NHLBI EVS (http://evs.gs.washington.edu/EVS/; accessed Jan 2014) datasets. The variant creates a BsrDI restriction site, which was used to screen for the presence of the variant allele in Pakistani controls by RFLP-PCR. The variant was not identified in 250 controls, in either heterozygous or homozygous form.

Linkage analysis across the 22q region using Simwalk2 a maximum location score (directly comparable to multipoint LOD score) of 6.197 was calculated for markers D22S280 and *DNAL4* (NM_005740): c.153+2T>C (Fig. 1d).

Screening of *DNAL4* for mutations in 13 MRMV cases from Canada showed no mutations in this cohort.

Comparative protein sequence analysis for DNAL4 using ClustalW2 alignment (http://www.ebi.ac.uk) shows it to be highly conserved across the kingdom Animalia (or Metazoa). Conservation is higher than 98 % identity across all mammalian species. Conservation appears to be particularly high across the deleted stretch of the protein (residues 24–51), with 54 % of residues conserved across all species, compared to 27 % for the rest of the protein (see Fig. 3).

Discussion

The data presented here show strong evidence that a splice site mutation in *DNAL4* is the causative mutation for MRMV in this family. Although next generation sequencing and Sanger sequencing were able to exclude coding mutations in all other genes at the linked and HBD locus on 22q13.1, the possibility of a causative mutation in untranslated regions, as well as intronic or intergenic regions could not be excluded by this approach. DNAL4 protein is believed to be part of the axonemal (or ciliary and flagellar) complex of dynein molecules (including dynein heavy and light chains) (GO:0005858), and a component of the microtubule-based dynein motor complex (Iwasaki et al. 2005). There are just two known axonemal light chain proteins, DNAL1 and DNAL4, which sit at the outer edge of the complex.

Axonemal dynein components are important for polarity. For example, in medaka (Japanese rice fish, *Oryzias latipes*), axonemal intermediate chain 2 (Dnai2) mutants show a defect in the left–right polarity of organs (Nagao et al. 2010). In humans, mutations in various dynein axonemal component genes, such as dynein axonemal assembly factor 2 (DNAAF2), or axonemal light chain gene, *DNAL1*, result in primary ciliary dyskinesis with or without *situs inversus* (Pennarun et al. 1999; Omran et al. 2008). Studies of dynein components in Chlamydomonas have shown that knockout of LC10, the orthologue of DNAL4, show only weak disruption of cilial/flagellar beat (Tanner et al. 2008). Immunostaining of murine tissues showed strong expression of DNAL4 in apical cilia in the bronchial epithelium, and in sperm flagella. In the mirror movement family reported here, there is no evidence of either *situs inversus*,

Table 2 Whole exome sequencing statistics from MRMV affected individual VI:2

	Annovar	DNASTAR: NGen
WES coverage		
Number of all variations	48580	68060
Number of homozygous variations	9169	29930
Mean coverage		25.25×
Median coverage		15×
% of variants with ≥10× coverage		67.63
% of variants with ≥20× coverage		38.28
WES variants		
Number of SNPs	48580	65510
Number of Indels		2550
Number of homozygous SNPs	9169	28704
Number of homozygous Indels		1226
Number of homozygous coding SNPs	9120	27547
Number of homozygous coding Indels		1180
Number of homozygous coding SNPs without rs number	589	1225
Number of homozygous coding Indels without rs number		290
Number of homozygous coding SNPs in HBD region	53	152
Number of homozygous coding Indels in HBD region		1
Number of homozygous coding SNPs in HBD region without rs number	4	6
Number of homozygous coding Indels in HBD region without rs number		0
Number of homozygous coding SNPs in HBD region on 22q13	55	42
Number of homozygous coding SNPs in HBD region on 22q13, excluding synonymous changes	31	23
Number of homozygous coding SNPs in HBD region on 22q13 with variant frequency ≤0.05, excluding synonymous changes	3	2
Number of non-neutral homozygous coding SNPs in HBD region on 22q13 with variant frequency ≤0.05, excluding synonymous changes	1	0

For *DNAL4* the HBD region is Chr22:36605976-39904648 (hg19). Variants with lower than 3× coverage were removed. For the Chr22 HBD region 609 exons showed adequate coverage (≥8×), and the 11 exons (1.8 %) not sufficiently covered were PCR amplified and Sanger sequenced. For the smaller HBD regions on chromosomes 5, 7, 8, 9, 10 and 16, 432 exons were adequately covered by WES (≥8×), and 10 exons (2.3 %) not sufficiently covered were checked by Sanger sequencing

or primary ciliary dyskinesis. Although sperm motility was not checked specifically, there is clearly no evidence of a fertility issue in this family. This suggests that DNAL4 may only play a minor ciliary/flagellar role. Data from the St. Jude Brain Gene Expression Map (BGEM: http://www.stjudebgem.org) in situ hybridization database (Magdaleno et al. 2006) suggest, somewhat surprisingly, that the *DNAL4* mouse ortholog, *Dnal4c*, is expressed at much higher levels than other dynein components in embryogenesis, and is prominently expressed in hippocampus, suggesting that DNAL4 may have additional functions unrelated to a role in the axoneme (Tanner et al. 2008). Data from the BioGPS database also show highest expression for mouse *Dnalc4* (array: Affymetrix MOE430, probe: 1416870_at) in testis, and then nucleus accumbens, and in humans, *DNAL4* is expressed highest in testis and thyroid, then in whole brain (array: Affymetrix U133A, probe: 204008_at).

Protein interaction analysis using the BioGRID data repository (Biological General Repository for Interaction Datasets; http://thebiogrid.org/) version 3.2.108 suggests interactions between DNAL4 and DYNLL2 (a cytoplasmic dynein light chain), FHL5, SCTR and GPBP1. Firstly, we note no reported interactions with other axonemal dynein components, yet a yeast-two-hybrid screening shows interaction with an 8 kDa cytoplasmic light chain LC8-type 2 dynein component, DYNLL2 (Rual et al. 2005). It is also of interest that BioGRID lists a number of interactions for DYNLL2, including a number of neuronal components such as DLG4 (known more commonly as PSD-95), DLG2, DLGAP1, SHANK2, HOMER3 and GPRIN2. Secondly, there appears to be no obvious direct interaction link between DNAL4 (or via DYNLL2) and RAD51, DCC or netrin-1 (NTN1). It has recently been demonstrated that DCC links netrin-1 signaling to microtubules via direct binding to the neuronal β-tubulin isoform TUBB3 (Qu et al. 2013). TUBB3 is a microtubule component, and is known to play a crucial role in axonal guidance. A recent study in drosophila showed that an 8 kDa cytoplasmic dynein

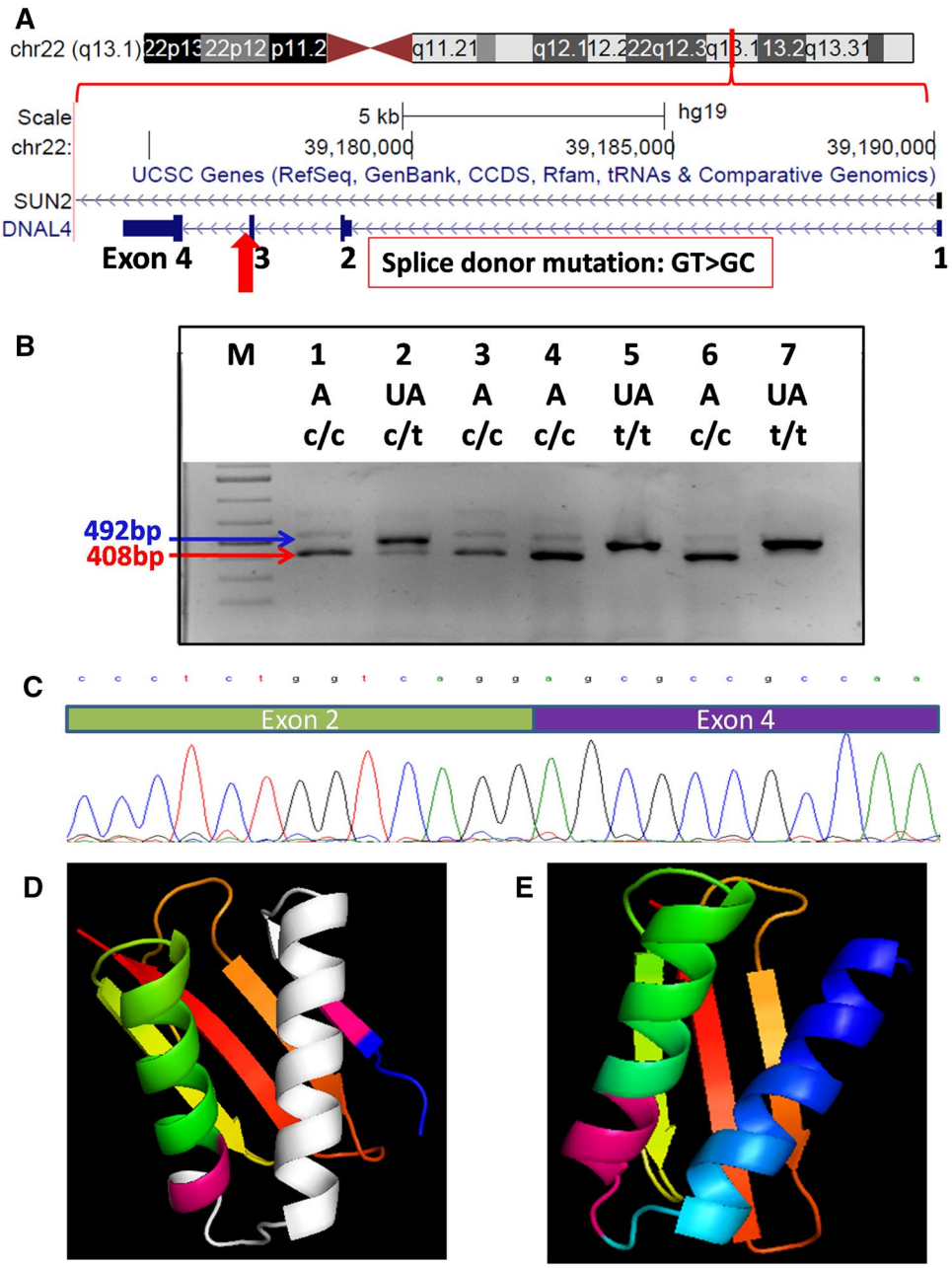

Fig. 2 **a** Ideogram of chromosome 22 indicating region of HBD, and the *DNAL4* gene, indicating the location of the NM_005740.2 c.153+2T>C variant at the exon 3/intron 3 splice site. **b** RT-PCR gel for DNAL4, spanning exons 1–4. *Lane M* contains size marker: Generuler 1 Kb ladder Plus (Fermentas); *lanes 1–3* from whole blood mRNA from V:15, III:5 and IV:7 respectively*; lanes 4–7* from lymphoblast mRNA from V:15, V:11, IV:7 and unrelated unaffected control. *A* affected, *UA* unaffected. Genotype for the c.153+2T>C variant is shown below affected status. **c** Ideogrammatic representation of the resulting spliced mRNA showing exclusion of exon3, and the electropherogram of the resulting RT-PCR sequence of the exon 2/exon 4 splice junction. **d** Predicted 3D structures for wild-type DNAL4, and **e** the mutant DNAL4 with the 28 amino acid stretch encoded by exon 3 missing. The *pink bars* represent the sequence flanking the 28 residue deletion section in the wild-type model and the mutant model

light chain protein is required for axonal guidance (Phillis et al. 1996). It was suggested in this study that disruption of dynein function could affect microtubule bundling, and thereby disrupt directional axonal growth. While DNAL4 is unlikely to bind directly to the microtubule assembly, it is very likely that the disruption of DNAL4 caused by the deletion of 28 amino acids would disrupt either homodimerization, or interactions with the dynein complex, possibly via DYNLL2, or interaction between the dynein complex and cargo molecules, which could ultimately result in disrupted axonal growth.

Gene ontology analysis also suggests a role for DNAL4 in the neurotrophin TRK receptor signaling pathway (GO:0048011), and neurotrophin signaling pathway (GO:0038179). The protein tyrosine phosphatase, non-receptor type 11 (PTPN11) is also present in the neurotrophin receptor pathways (GO:0048011 and GO:0038179), and is also included in the axogenesis pathway (GO:0007409) along with NTN1 and DCC. So, PTPN11 activity may represent a common link between DCC/netrin and DNAL4.

Performing unilateral movements requires communication between cortical and subcortical regions spanning the brain hemispheres—mainly through the corpus callosum—that are necessary to restrict output to the primary motor cortex (M1) contralateral to the intended hand movement

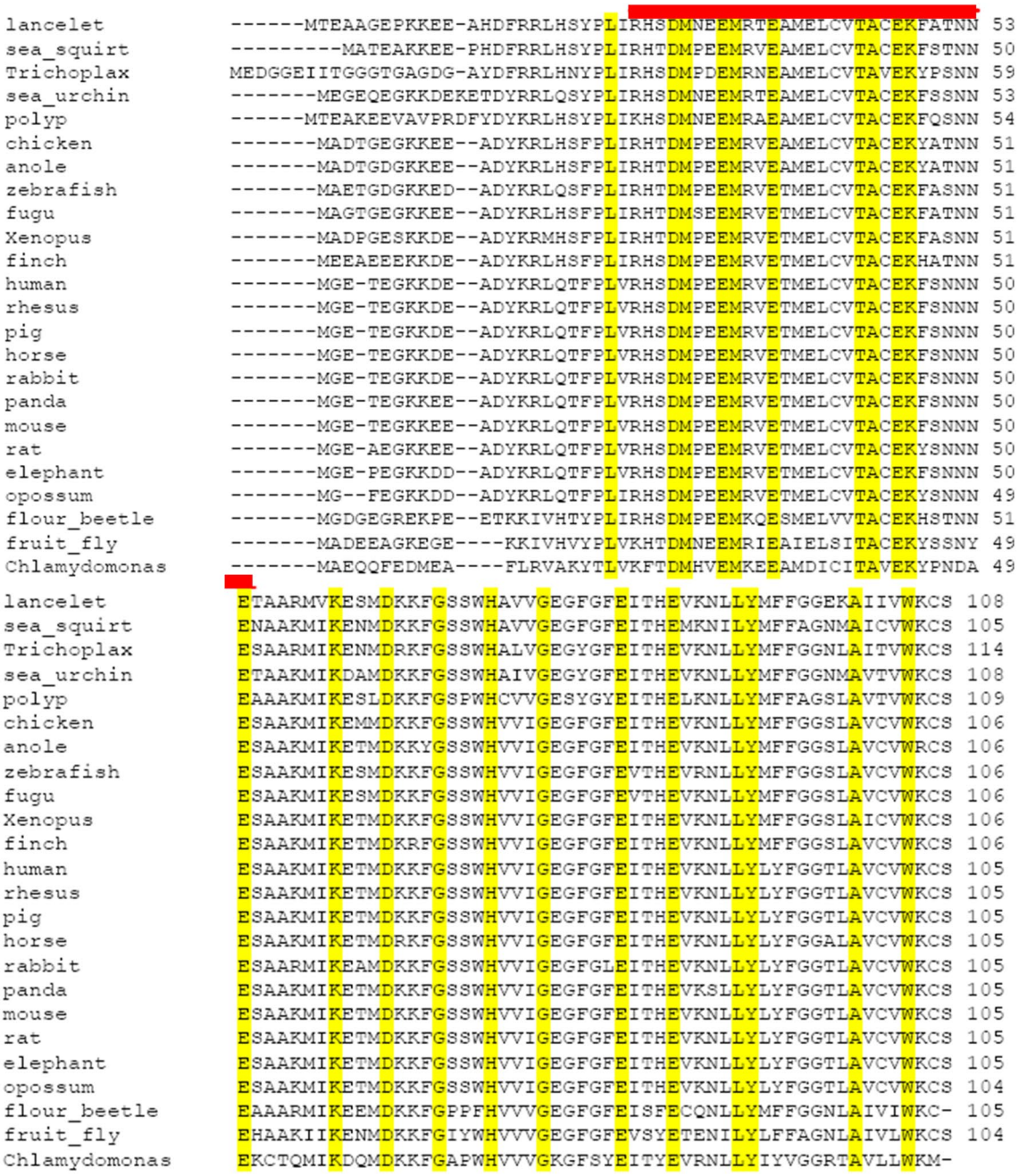

Fig. 3 Analysis of evolutionary conservation of DNAL4 protein using ClustalW2 alignment. The *red bar* above the alignment indicates the position of the 28 deleted amino acids. *Yellow shading* indicates amino acids that are conserved 100 % across the species included in the alignment. Protein sequences used: human NP_005731.1; rhesus NP_001247540.1; pig NP_001231596.1; elephant XP_003419805.1; giant panda XP_002914599.1; horse XP_005606702.1; mouse NP_059498.2; rat NP_001009666.1; rabbit XP_002711436.1; opossum XP_001367599.1; chicken NP_001006242.1; finch XP_005421907.1; anole XP_003221024.1; *Xenopus* NP_001087464.1; zebrafish NP_001003603.1; fugu XP_003976859.1; lancelet XP_002595410.1; sea squirt XP_002126866.1; hydra XP_002162246.1; sea urchin XP_794465.1; *Trichloplax* XP_002110087.1; flour beetle XP_967210.1; fruit fly NP_610734.1; *Chlamydomonas* ACC68802.1

(reviewed in Beaulé et al. 2012). Modulation of transcallosal interhemispheric inhibition is necessary to suppress mirroring, and the corpus callosum is believed to play a crucial role. The network of cortical and subcortical areas that are required for performing unilateral movements is known as the nonmirroring network, and it is believed that this area involves the supplementary motor area (SMA), dorsal premotor cortex (dPMC), the ipsilateral motor cortex

(M1), and the basal ganglia, and disruption of any part of this network may increase the tendency towards symmetrical mirrored hand movements (reviewed in Beaulé et al. 2012). We suggest that the *DNAL4* mutation identified in the Pakistani MRMV family leads to inability of DNAL4 either to homodimerize or to bind to DYNLL2, and therefore disrupting the function of DYNLL2, and thus the overall dynein complex, in retrograde transport required for netrin-1-induced axon outgrowth and pathfinding during development, either within commissural callosal regions, or within the nonmirroring network.

Acknowledgments We wish to thank the family members for their willing participation and cooperation with this study. This research was supported by a grant from the Canadian Institutes of Health Research (#MOP-102758), and by the Pakistan Higher Education Commission (HEC). We declare that the authors have no competing interests for this article.

References

Beaulé V, Tremblay S, Theoret H (2012) Interhemispheric control of unilateral movement. Neural Plast 2012:627816. doi:10.1155/2012/627816

Bonnet C, Roubertie A, Doummar D, Bahi-Buisson N, Cochen de Cock V, Roze E (2010) Developmental and benign movement disorders in childhood. Mov Disord 25:1317–1334. doi:10.1002/mds.22944

Cincotta M, Borgheresi A, Balzini L, Vannucchi L, Zeloni G, Ragazzoni A, Benvenuti F, Zaccara G, Arnetoli G, Ziemann U (2003) Separate ipsilateral and contralateral corticospinal projections in congenital mirror movements: neurophysiological evidence and significance for motor rehabilitation. Mov Disord 18:1294–1300

Cohen LG, Meer J, Tarkka I, Bierner S, Leiderman DB, Dubinsky RM, Sanes JN, Jabbari B, Branscum B, Hallett M (1991) Congenital mirror movements. Abnormal organization of motor pathways in two patients. Brain 114:381–403

David M, Dzamba M, Lister D, Ilie L, Brudno M (2011) SHRiMP2: sensitive yet practical short read mapping. Bioinformatics 27:1011–2101. doi:10.1093/bioinformatics/btr046

Depienne C, Cincotta M, Billot S, Bouteiller D, Groppa S, Brochard V, Flamand C, Hubsch C, Meunier S, Giovannelli F, Klebe S, Corvol JC, Vidailhet M, Brice A, Roze E (2011) A novel DCC mutation and genetic heterogeneity in congenital mirror movements. Neurology 76:260–264. doi:10.1212/WNL.0b013e318207b1e0

Depienne C, Bouteiller D, Meneret A, Billot S, Groppa S, Klebe S, Charbonnier-Beaupel F, Corvol JC, Saraiva JP, Brueggemann N, Bhatia K, Cincotta M, Brochard V, Flamand-Roze C, Carpentier W, Meunier S, Marie Y, Gaussen M, Stevanin G, Wehrle R, Vidailhet M, Klein C, Dusart I, Brice A, Roze E (2012) RAD51 haploinsufficiency causes congenital mirror movements in humans. Am J Hum Genet 90:301–307. doi:10.1016/j.ajhg.2011.12.002

Gallea C, Popa T, Hubsch C, Valabregue R, Brochard V, Kundu P, Schmitt B, Bardinet E, Bertasi E, Flamand-Roze C, Alexandre N, Delmaire C, Méneret A, Depienne C, Poupon C, Hertz-Pannier L, Cincotta M, Vidailhet M, Lehericy S, Meunier S, Roze E (2013) RAD51 deficiency disrupts the corticospinal lateralization of motor control. Brain 136:3333–3346. doi:10.1093/brain/awt258

Galléa C, Popa T, Billot S, Méneret A, Depienne C, Roze E (2011) Congenital mirror movements: a clue to understanding bimanual motor control. J Neurol 258:1911–1919. doi:10.1007/s00415-011-6107-9

González-Pérez A, López-Bigas N (2011) Improving the assessment of the outcome of nonsynonymous SNVs with a Consensus Deleteriousness Score, Condel. Am J Hum Genet 88:440–449. doi:10.1016/j.ajhg.2011.03.004

Homer N, Nelson SF (2010) Improved variant discovery through local re-alignment of short-read next-generation sequencing data using SRMA. Genome Biol 11:R99. doi:10.1186/gb-2010-11-10-r99

Iwasaki M, Kuwata T, Yamazaki Y, Jenkins NA, Copeland NG, Osato M, Ito Y, Kroon E, Sauvageau G, Nakamura T (2005) Identification of cooperative genes for NUP98-HOXA9 in myeloid leukemogenesis using a mouse model. Blood 105:784–793

Lahiri DK, Bye S, Nurnberger JI Jr, Hodes ME, Crisp M (1992) A non-organic and non-enzymatic extraction method gives higher yields of genomic DNA from whole-blood samples than do nine other methods tested. J Biochem Biophys Methods 25:193–205

Magdaleno S, Jensen P, Brumwell CL, Seal A, Lehman K, Asbury A, Cheung T, Cornelius T, Batten DM, Eden C, Norland SM, Rice DS, Dosooye N, Shakya S, Mehta P, Curran T (2006) BGEM: an in situ hybridization database of gene expression in the embryonic and adult mouse nervous system. PLoS Biol 4:e86

McKenna A, Hanna M, Banks E, Sivachenko A, Cibulskis K, Kernytsky A, Garimella K, Altshuler D, Gabriel S, Daly M, DePristo MA (2010) The genome analysis toolkit: a MapReduce framework for analyzing next-generation DNA sequencing data. Genome Res 20:1297–1303. doi:10.1101/gr.107524.110

Nagao Y, Cheng J, Kamura K, Seki R, Maeda A, Nihei D, Koshida S, Wakamatsu Y, Fujimoto T, Hibi M, Hashimoto H (2010) Dynein axonemal intermediate chain 2 is required for formation of the left–right body axis and kidney in medaka. Dev Biol 347:53–61. doi:10.1016/j.ydbio.2010.08.001

Omran H, Kobayashi D, Olbrich H, Tsukahara T, Loges NT, Hagiwara H, Zhang Q, Leblond G, O'Toole E, Hara C, Mizuno H, Kawano H, Fliegauf M, Yagi T, Koshida S, Miyawaki A, Zentgraf H, Seithe H, Reinhardt R, Watanabe Y, Kamiya R, Mitchell DR, Takeda H (2008) Ktu/PF13 is required for cytoplasmic pre-assembly of axonemal dyneins. Nature 456:611–616. doi:10.1038/nature07471

Pennarun G, Escudier E, Chapelin C, Bridoux A-M, Cacheux V, Roger G, Clement A, Goossens M, Amselem S, Duriez B (1999) Loss-of-function mutations in a human gene related to *Chlamydomonas reinhardtii* dynein IC78 result in primary ciliary dyskinesia. Am J Hum Genet 65:1508–1519

Phillis R, Statton D, Caruccio P, Murphey RK (1996) Mutations in the 8 kDa dynein light chain gene disrupt sensory axon projections in the Drosophila imaginal CNS. Development 122:2955–2963

Qu C, Dwyer T, Shao Q, Yang T, Huang H, Liu G (2013) Direct binding of TUBB3 with DCC couples netrin-1 signaling to intracellular microtubule dynamics in axon outgrowth and guidance. J Cell Sci 126:3070–3081. doi:10.1242/jcs.122184

Rasmussen P (1993) Persistent mirror movement. A clinical study of 17 children, adolescents and young adults. Dev Med Child Neurol 35:699–707

Regli F, Filippa G, Wiesendanger M (1967) Hereditary mirror movements. Arch Neurol 16:620–623

Rual JF, Venkatesan K, Hao T, Hirozane-Kishikawa T, Dricot A, Li N, Berriz GF, Gibbons FD, Dreze M, Ayivi-Guedehoussou N, Klitgord N, Simon C, Boxem M, Milstein S, Rosenberg J, Goldberg DS, Zhang LV, Wong SL, Franklin G, Li S, Albala JS, Lim J, Fraughton C, Llamosas E, Cevik S, Bex C, Lamesch P, Sikorski RS, Vandenhaute J, Zoghbi HY, Smolyar A, Bosak S, Sequerra R, Doucette-Stamm L, Cusick ME, Hill DE, Roth FP, Vidal M (2005) Towards a proteome-scale map of the human protein–protein interaction network. Nature 437:1173–1178

Seelow D, Schuelke M, Hildebrandt F, Nürnberg P (2009) HomozygosityMapper—an interactive approach to homozygosity mapping. Nucleic Acids Res 37(Web Server issue):W593–W599. doi:10.1093/nar/gkp369

Sobel E, Lange K (1996) Descent graphs in pedigree analysis: applications to haplotyping, location scores, and marker sharing statistics. Am J Hum Genet 58:1323–1337

Sobel E, Sengul H, Weeks DE (2001) Multipoint estimation of identity-by-descent probabilities at arbitrary positions among marker loci on general pedigrees. Hum Hered 52:121–131

Sobel E, Papp JC, Lange K (2002) Detection and integration of genotyping errors in statistical genetics. Am J Hum Genet 70:496–508

Srour M, Philibert M, Dion MH, Duquette A, Richer F, Rouleau GA, Chouinard S (2009) Familial congenital mirror movements: report of a large 4-generation family. Neurology 73:729–731. doi:10.1212/WNL.0b013e3181b59bda

Srour M, Riviére JB, Pham JM, Dubé MP, Girard S, Morin S, Dion PA, Asselin G, Rochefort D, Hince P, Diab S, Sharafaddinzadeh N, Chouinard S, Théoret H, Charron F, Rouleau GA (2010) Mutations in DCC cause congenital mirror movements. Science 328:592. doi:10.1126/science.1186463

Tanner CA, Rompolas P, Patel-King RS, Gorbatyuk O, Wakabayashi K, Pazour GJ, King SM (2008) Three members of the LC8/DYNLL family are required for outer arm dynein motor function. Mol Biol Cell 19:3724–3734. doi:10.1091/mbc.E08-04-0362

Tcherkezian J, Brittis PA, Thomas F, Roux PP, Flanagan JG (2010) Transmembrane receptor DCC associates with protein synthesis machinery and regulates translation. Cell 141:632–644. doi:10.1016/j.cell.2010.04.008

Wang K, Li M, Hakonarson H (2010) ANNOVAR: functional annotation of genetic variants from high-throughput sequencing data. Nucleic Acids Res 38:e164. doi:10.1093/nar/gkq603